PMHDO-*g*-PEG Double-Bond-Based Amphiphilic Graft Copolymer: Synthesis and Diverse Self-Assembled Nanostructures

Xiaohuan Zhang,[†] Zhong Shen,[†,§] Chun Feng,[†] Dong Yang,[‡] Yaogong Li,[†] Jianhua Hu,*,[‡] Guolin Lu,[†] and Xiaoyu Huang*,[†]

[†]*Key Laboratory of Organofluorine Chemistry and Laboratory of Polymer Materials, Shanghai Institute of Organic Chemistry, Chinese Academy of Sciences, 345 Lingling Road, Shanghai 200032, P. R. China, and* [‡]*Key Laboratory of Molecular Engineering of Polymers (Ministry of Education), Laboratory of Advanced Materials and Department of Macromolecular Science, Fudan University, 220 Handan Road, Shanghai 200433, P. R. China.* [§] *Now working at Evonik Degussa GmbH*

ABSTRACT: Self-assembly behavior of a double-bond-based amphiphilic graft copolymer consisting of hydrophobic polyallene backbone and hydrophilic poly(ethylene glycol) side chains in tetrahydrofuran (THF)/water was investigated. Polyallene backbone was first prepared via living coordination polymerization of 6-methyl-1,2-heptadien-4-ol (MHDO) initiated by $[(\eta^3\text{-allyl})\text{NiOCOCF}_3]_2$. The targeted amphiphilic graft copolymer with relative narrow molecular weight distribution ($M_w/M_n = 1.22$) was synthesized by the coupling reaction between the pendant hydroxyls of the backbone and acyl chloride end group of poly (ethylene glycol) via the grafting-onto approach. The critical micelle concentration (cmc) was determined by the fluorescence probe technique. Micelle morphologies could be well tuned by water content, initial copolymer content, and ion strength. In particular, this kind of achiral copolymer could aggregate to form chiral helical nanostructures under given conditions.

Introduction

The self-assembly behavior of amphiphilic copolymers in aqueous media has been extensively studied for decades[1,2] due to their special physicochemical properties and self-assembly morphologies which led to potential applications in many fields including the solubilizer,[3] drug delivery,[4−7] catalysis,[8] and microelectronics.[9,10] The self-assembly behavior of amphiphilic copolymer with a given chemical structure in aqueous media is influenced by many experimental parameters such as pH value, ionic strength of the solution, micelle preparation conditions, concentration, molecular weight, and composition of the copolymer.[11−13] On the other hand, the most prominent advantage of amphiphilic copolymer is the wide variability of chemical structure.[14] A fresh amphiphilic copolymer with novel chemical structure and molecular architecture is supposed to show new and interesting self-assembly behaviors, which is significant in understanding the structure−property correlation and exploring new materials.[15]

Most of previous researches focused on the self-assembly behavior of amphiphilic "block" copolymers, and only a few researches touched on the self-assembly behavior of amphiphilic "graft" copolymers.[16] Graft copolymers possess additional complexity in self-assembly due to their complicated and confined structures,[17−19] which can provide more information about the control of micellar morphologies and the design of new nanomaterials. However, synthetic difficulties limited the studies on the self-assembly behavior of graft copolymers.

Generally, polymer chemists employed three strategies[20] including grafting-through,[21,22] grafting-from,[23] and grafting-onto to synthesize graft copolymers. The development of ATRP,[24−26] SET-LRP,[27] and RAFT[28] has made it feasible to prepare the versatile well-defined comb copolymers from the grafting-through[29−31] and grafting-from strategies.[32] The grafting-onto method is to attach side chains into the backbone by a coupling reaction.[33] Both backbone and side chains can be prepared and characterized independently. This technique is often applied when the coupling efficiency is high enough.

Allene derivatives have cumulated double bonds so that they can be regarded as the isomers of propargyl derivatives. Utilizing this structure characteristic, a kind of polymer possessing reactive exomethylene substituents directly linked to the main chain can be obtained when either part (1,2- or 2,3-) of cumulated double bonds is selectively polymerized. Many approaches have been used for the polymerization of allene derivatives.[34] Since the controllability of radical or cationic polymerization was poor, living coordination polymerization of allene derivatives was developed using $[(\eta^3\text{-allyl})\text{NiOCOCF}_3]_2$ as initiator.[35−39] Moreover, the reactive pendant group such as hydroxyl can be kept for the following modification.[38] However, most kinds of copolymers containing polyallene segment cannot be synthesized by this kind of nickel-catalyzed living polymerization because $[(\eta^3\text{-allyl})\text{NiOCOCF}_3]_2$ can only initiate the polymerization of butadiene and its derivatives, isocyano monomers, and allene derivatives. Furthermore, none has reported self-assembly behavior of amphiphilic block or graft copolymers bearing polyallene segment.

In our previous studies, we have utilized the graft-from approach to synthesize hydrophobic graft copolymers containing polyallene backbone via the combination of living coordination polymerization and ATRP.[40−42] In this work, the purpose is to study the self-assembly behavior of polyallene-based amphiphilic graft copolymer. Poly(6-methyl-1,2-heptadien-4-ol) (PMHDO) bearing hydroxyls was first prepared by nickel-catalyzed living coordination polymerization. Pendant hydroxyls of the backbone reacted with acyl chloride end group of poly(ethylene glycol) (PEG) to give the targeted amphiphilic graft copolymer by grafting-onto strategy (Scheme 1). The cmc was determined

*To whom correspondence should be addressed. E-mail: hujh@fudan.edu.cn (J.H.); xyhuang@mail.sioc.ac.cn (X.H.).

Scheme 1. Synthesis of Polyallene-Based Amphiphilic Graft Copolymer
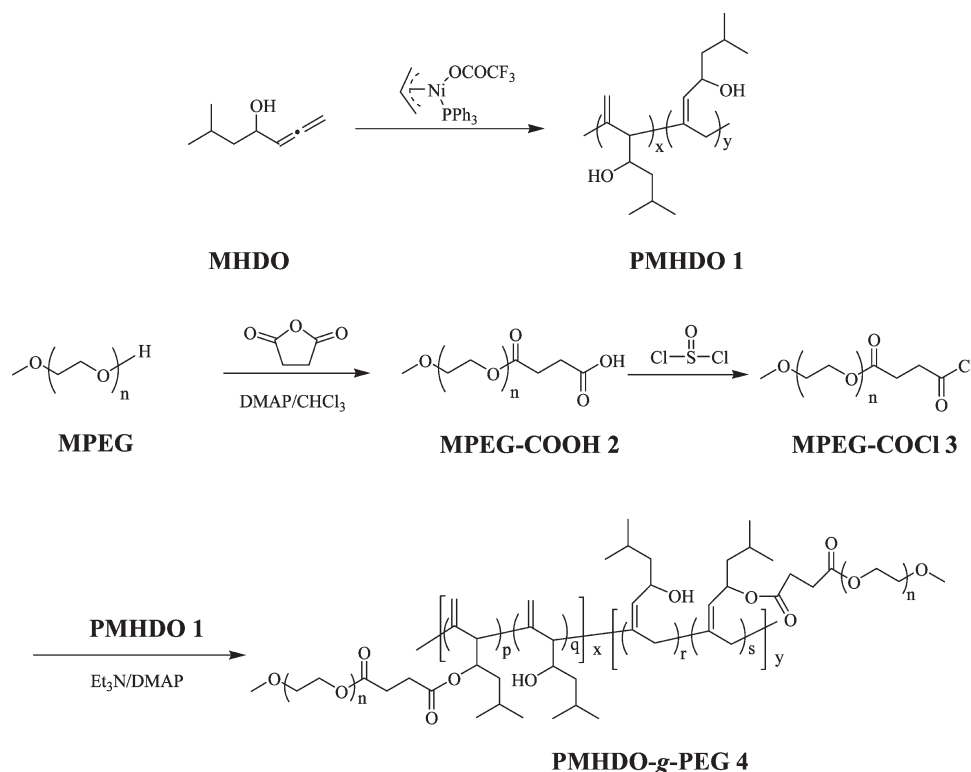
by fluorescence spectroscopy using *N*-phenyl-1-naphthylamine as probe. Transmission electron microscopy (TEM) showed various self-assembled micelle morphologies with the changing of experiment parameters.

Experimental Section

Materials. Poly(ethylene glycol) monomethyl ether (MPEG, M_n = 350, Alfa Aesar) was dried azeotropically with toluene followed by drying in vacuo and stored over 4 Å molecular sieve. Toluene (Aldrich, 99.5%) was dried over CaH_2 for several days and distilled from sodium and benzophenone under N_2 prior to use. *N*-Phenyl-1-naphthylamine (PNA, Alfa Aesar, 97%) was purified by recrystallization in ethanol for three times. Allyl trifluoroacetate (Aldrich, 98%) was redistilled prior to use. PPh_3 (Acros, 99%) was recrystallized with CH_2Cl_2/hexane. 6-Methyl-1,2-heptadiene-4-ol (MHDO) was synthesized according to previous literature.[43] Bis(1,5-cyclooctadiene)nickel(0) (Ni(COD)$_2$, Aldrich), 4-di(methylamino)pyridine (DMAP, Aldrich, 99%), succinic anhydride (Aldrich, 99%), thionyl chloride (SOCl$_2$, Aldrich, 99.5%), and triethylamine (Et$_3$N, Aldrich, 99.5%) were used as received.

Measurements. FT-IR spectra were recorded on a Nicolet AVATAR-360 FT-IR spectrophotometer with 4 cm^{-1} resolution. All NMR analyses were performed on a Bruker Avance 500 spectrometer (500 MHz) in CDCl$_3$; TMS (^{1}H NMR) and CDCl$_3$ (^{13}C NMR) were used as internal standards. Relative molecular weight and molecular weight distribution were measured by conventional gel permeation chromatography (GPC) system equipped with a Waters 1515 Isocratic HPLC pump, a Waters 2414 refractive index detector, and a set of Waters Styragel columns (HR3, HR4, and HR5, 7.8 × 300 mm). GPC measurements were run at 35 °C using THF as eluent with a flow rate of 1.0 mL/min, and the system was calibrated with linear polystyrene standards. Absolute molecular weight of graft copolymer was determined by GPC equipped with a multiangle light scattering detector (GPC/MALS) using THF as eluent; detectors: Wyatt Optilab rEX refractive index detector and Wyatt DAWN HELEOS 18-angle light

scattering detector with a 50 mW solid-state laser operating at 658 nm. Steady-state fluorescence spectra of PNA were measured on a Hitachi FL-4500 spectrofluorometer with the bandwidth of 5 nm for excitation and emission; the emission intensity at 418 nm was recorded to determine the cmc with a λ_{ex} = 340 nm. TEM images were obtained by a JEOL JEM-1230 instrument operated at 80 kV. Circular dichroism (CD) was measured by a JASCO J-810 chiropitical spectrometer.

Living Coordination Homopolymerization of MHDO. PMHDO **1** homopolymer was prepared via living coordination polymerization of MHDO initiated by [(η^3-allyl)NiOCOCF$_3$]$_2$ under N_2 at 50 °C. To a 25 mL Schlenk flask (flame-dried under vacuum prior to use) sealed with a rubber septum, Ni(COD)$_2$ (0.1001 g, 0.3635 mmol), allyl trifluoroacetate (0.05 mL, 0.3635 mmol), and toluene (14 mL) were charged. The mixture reacted under N_2 at room temperature for 20 min. Next, PPh$_3$ (1.0 M in toluene, 0.37 mL, 0.37 mmol) and MHDO (2.2 mL, 14.42 mmol) were introduced via a gastight syringe at 0 °C. The flask was immersed into an oil bath thermostated at 50 °C to start the polymerization. The polymerization lasted for 3 h. The solution was precipitated in cold *n*-hexane. After repeated purification by dissolving in THF and precipitating in cold *n*-hexane, 1.5500 g of PMHDO **1** was obtained with a yield of 85.2%. GPC: M_n = 5700 g/mol, M_w/M_n = 1.17. FT-IR: ν (cm^{-1}): 3401, 2956, 2919, 2869, 1640, 1468, 1367, 1048. ^{1}H NMR: δ (ppm): 0.90 (6H, −CH(CH$_3$)$_2$), 1.25−2.00 (3H, −CH$_2$CH(CH$_3$)$_2$), 2.34 (2H × *y*, =C−CH$_2$−C=), 2.88 (1H × *x*, =C−CH−C=), 3.60 (1H × *x*, $\rangle$CH−OH), 4.40 (1H × *y*, $\rangle$CH−OH), 4.80−6.00 (2H × *x*, =CH$_2$ and 1H × *y*, −CH=). ^{13}C NMR: δ (ppm): 23.3, 24.5, 47.2, 66.7, 113.8, 132.6, 141.0, 147.3.

Functionalization of MPEG. α-Monocarboxy-ω-monomethoxy poly(ethylene glycol), MPEG-COOH **2**, was prepared by reacting MPEG with succinic anhydride catalyzed by DMAP according to previous literatures.[44,45] FT-IR: ν (film, cm^{-1}): 3451, 2880, 1736, 1450, 1355, 1241, 1100, 949, 845. ^{1}H NMR: δ (ppm): 2.64 (4H, COCH$_2$CH$_2$CO), 3.37 (3H, OCH$_3$), 3.55 (2H, COOCH$_2$CH$_2$O), 3.64 (4H, OCH$_2$CH$_2$), 4.26 (2H,

COOCH_2CH$_2$). ^{13}C NMR: δ (ppm): 29.0, 59.0, 63.9, 69.0, 70.5, 71.9, 172.3 (*C*OOCH$_2$CH$_2$), 175.3 (*C*OOH).

MPEG-COOH **2** was treated with SOCl$_2$ to convert carboxyl end group to acyl chloride end group. MPEG-COOH **2** (0.36 g, 0.789 mmol of carboxyl) and SOCl$_2$ (5 mL) were added to a 25 mL three-neck flask (flame-dried under vacuum prior to use) under N$_2$. The reaction lasted for 2 h at room temperature. Excessive SOCl$_2$ was removed under vacuum. The crude product was dried in vacuo to obtain MPEG-COCl **3** for next reaction without further purification.

Coupling Reaction between PMHDO 1 and MPEG-COCl 3. To a 100 mL three-neck flask (flame-dried under vacuum prior to use), PMHDO **1** (100.0 mg, M_n = 5700 g/mol, M_w/M_n = 1.17, 0.793 mmol of hydroxyl) and DMAP (11.2 mg, 0.0920 mmol) were added under N$_2$. Dry THF (20 mL) and Et$_3$N (0.11 mL, 0.789 mmol) were introduced via a gastight syringe. The mixture was cooled to 0 °C, and the freshly prepared MPEG-COCl **3** (0.789 mmol of acyl chloride group) in 10 mL of dry THF was added slowly. The mixture was stirred at 0 °C for 1 h followed by stirring at room temperature for another 24 h. The reaction was quenched by adding brine, and the aqueous phase was extracted with THF for two times. The combined organic phase was concentrated, and the crude product was dissolved in chloroform. The solution was washed with distilled water for three times to remove the unreacted MPEG-COCl **3**. The organic phase was dried against Na$_2$SO$_4$ overnight. After filtration, the solution was concentrated and precipitated into cold *n*-hexane. Finally, 0.153 g of PMHDO-*g*-PEG **4** was obtained as a yellowish viscous liquid after drying in vacuo. GPC: M_n = 8200 g/mol, M_w/M_n = 1.22. GPC-MALS: M_w = 15 000 g/mol, dn/dc = 0.100 mL/g. FT-IR: ν (cm^{-1}): 3451, 2955, 2932, 2865, 1734, 1640, 1472, 1363, 1344, 1254, 1136, 1113, 1042, 952, 852, 835, 801. ^{1}H NMR: δ (ppm): 0.88 (6H,CH(CH_3)$_2$), 1.10−2.00 (3H, CH_2CH-(CH$_3$)$_2$), 2.34 (2H × y, =C−CH_2−C=), 2.31 (1H × x,)CH−), 2.62 (4H, COCH_2CH_2CO), 2.88 (1H × x, =C−CH−C=), 3.37 (3H, OCH_3), 3.54 (2H, COOCH$_2$CH_2O and 1H × x,)CH−OH), 3.64 (4H, OCH_2CH_2), 4.21 (2H, COOCH_2CH$_2$), 4.35 (1H × y,)CH−OH and 1H × x,)CH−OCO−), 4.80−6.00 (1H × y,)CH−OCO−, 2H × x, =CH_2 and 1H × y, −CH=). ^{13}C NMR: δ (ppm): 22.4, 24.4, 28.3, 29.3, 44.4, 46.9, 58.8, 63.7, 66.4, 68.9, 70.4, 71.8, 112.9, 132.2, 172.4.

Determination of Critical Micelle Concentration. PNA was used as fluorescence probe to measure the cmc of PMHDO-*g*-PEG **4** graft copolymer in aqueous media. Acetone solution of PNA (1 mmol/L) was added to a large amount of water until the concentration of PNA reached 2 × 10^{-6} mol/L. Next, different amounts of THF solutions of PMHDO-*g*-PEG **4** graft copolymer (10, 0.1, or 0.001 mg/mL) were added to water containing PNA ([PNA] = 2 × 10^{-6} mol/L). The concentration of PMHDO-*g*-PEG **4** graft copolymer ranged from 1.0 × 10^{-6} to 1 mg/mL. All fluorescence spectra were recorded at 25 °C.

TEM Images. Micelle solution was prepared by adding water to THF solution of graft copolymer. PMHDO-*g*-PEG **4** graft copolymer was first dissolved in THF with different concentrations (0.1−1.6 wt %). Next, deionized water was added slowly (0.36 mL/h) to 1 g of THF stock solution until the desired water content was reached. The solution was sealed with a PTFE plug for equilibration under stirring for another 12 h. The solution was dialyzed against deionized water with slow stirring for 5 days to remove THF, and deionized water was changed twice a day. For TEM studies, a drop of micellar solution was deposited on an electron microscopy copper grid coated with carbon film and the water evaporated at room temperature.

Results and Discussion

Characterization of PMHDO Backbone and Functionalized MPEG. Nickel-catalyzed living coordination polymerization of MHDO was performed in the presence of PPh$_3$ at 50 °C using toluene as solvent, and this homopolymerization was complete in 3 h with a high yield of 85.2%. PMHDO **1** homopolymer was characterized by FT-IR, ^{1}H NMR, and
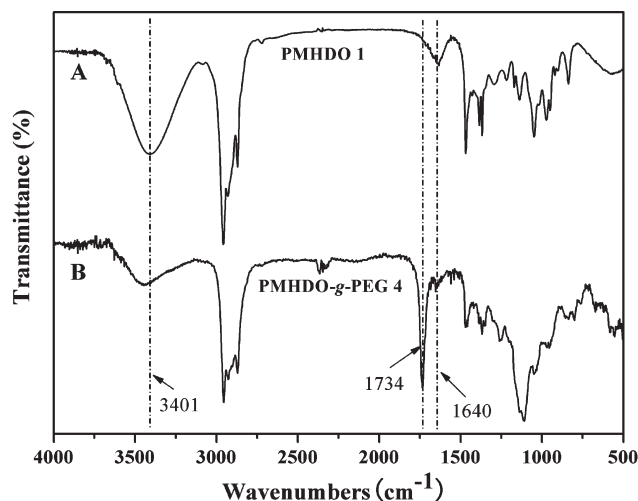

Figure 1. FT-IR spectra of PMHDO **1** (A) and PMHDO-*g*-PEG **4** (B).

^{13}C NMR. The peaks of hydroxyl and double bond appeared at 3401 and 1640 cm^{-1} in FT-IR spectrum of PMHDO **1** (Figure 1A), respectively. The chemical structure of PMHDO **1** was also affirmed by the broad peak between 4.80 and 6.00 ppm attributed to the protons of double bond in ^{1}H NMR spectrum and the signals of the carbons of double bond at 113.8, 132.6, 141.0, and 147.3 ppm in the ^{13}C NMR spectrum. PMHDO **1** homopolymer consisted of both 1,2- and 2,3-polymerized units (labeled y and x in Scheme 1), and the ratio of 1,2-polymerized units to 2,3-polymerized units can be evaluated from the integration area ratio of the peak at 4.40 ppm to the peak at 3.70 ppm. The result is 60:40, which meant PMHDO **1** contained 60% of 1,2-polymerized units and 40% of 2,3-polymerized units. All this evidence assured the formation of PMHDO homopolymer. Moreover, the living nature of nickel-catalyzed living coordination polymerization was demonstrated by the result of GPC since the molecular weight distribution of PMHDO is as narrow as 1.17, and the evolution of the molecular weights of PMHDO homopolymers with narrow molecular weight distributions increased linearly with the increasing of the feed ratios of the monomer to the initiator in earlier reports.[40−42] From the data of molecular weight (M_n = 5700 g/mol), we can estimate that every PMHDO chain has 45 repeating units. PMHDO is soluble in common organic solvents such as THF, CH$_2$Cl$_2$, DMSO, and acetone; however, it is insoluble in water.

The existence of a carboxyl end group in MPEG-COOH **2** was confirmed by a broad absorbance peak ranging from 2800 to 3500 cm^{-1} in FT-IR spectrum; meanwhile, a sharp peak attributed to carbonyl appeared at 1736 cm^{-1}. Two new peaks appeared at 2.64 and 4.26 ppm in the ^{1}H NMR spectrum of MPEG-COOH **2** (Figure 2A) in comparison with that of MPEG. The peaks "e" (2.64 ppm) and "d" (4.26 ppm) corresponded to four protons of −COCH_2CH_2-COOH and two protons of −COOCH_2CH$_2$O, respectively. The integration area ratio of peak "a" at 3.36 ppm to peak "d" at 4.26 ppm is 3:2, which is a clear evidence of complete transformation of monohydroxyl end group of MPEG. Moreover, new signals of the carbons of −COCH$_2$CH$_2$-CO$_2$H were found to locate at 29.0, 172.3, and 175.3 ppm in the ^{13}C NMR spectrum (Figure 2B), evidencing the successful introduction of carboxyl.

Synthesis of PMHDO-*g*-PEG Graft Copolymer. The esterification of pendant hydroxyls of PMHDO was first catalyzed by the DMAP/DCC system. However, it was very difficult to completely remove the side product of
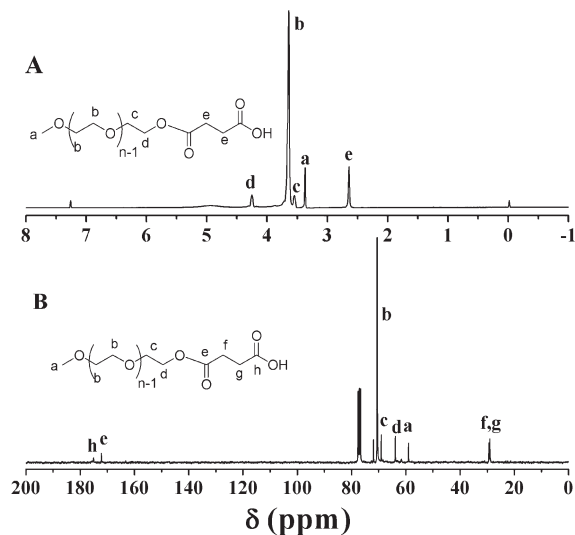
Figure 2. ^{1}H NMR (A) and ^{13}C NMR (B) spectra of MPEG-COOH **2** in CDCl$_3$.

N,N'-dicyclohexylurea. Different approaches such as precipitation, dialysis, and chromatography were tried, but in any case, the signals of byproduct remained in the ^{1}H NMR spectrum of purified product. Therefore, an alternative route was used to transform carboxyl end group of MPEG-COOH **2** into acyl chloride end group after reacting with SOCl$_2$. Pure PMHDO-*g*-PEG **4** graft copolymer was obtained after coupling reaction between the pendant hydroxyls of PMHDO and acyl chloride end group of functionalized MPEG catalyzed by DMAP in the presence of Et$_3$N.

PMHDO-*g*-PEG **4** graft copolymer showed a unimodal and symmetrical GPC curve, and its molecular weight distribution kept relatively narrow (M_w/M_n = 1.22). Moreover, the trace of functionalized MPEG was not found in the curve, which indicated that unreacted functionalized MPEG was removed entirely. The structure of graft copolymer was characterized by FT-IR, ^{1}H NMR, and ^{13}C NMR. The stretching peak of pendant hydroxyl around 3401 cm^{-1} became weaker, and a new strong peak attributed to carbonyl appeared at 1734 cm^{-1} in the FT-IR spectrum (Figure 1B) compared to that of PMHDO **1**. Furthermore, the peak of the double bond still appeared at 1640 cm^{-1} after esterification with MPEG-COCl **3**. Figure 3 shows the ^{1}H NMR spectrum of PMHDO-*g*-PEG **4**. Characteristic signals of corresponding protons of PMHDO backbone and PEG side chains appeared at 4.80−6.00 ppm (double bond) and 3.64 ppm (OCH_2CH_2), respectively. The signals of the corresponding carbons of backbone and side chains were also found in the ^{13}C NMR spectrum, as shown in Figure 4. The peaks at 112.9 and 132.2 ppm were attributed to double bonds of the backbone. The signals at 68.9 and 70.4 ppm demonstrated the presence of PEG side chains. In particular, a new peak at 172.4 ppm (OCOCH_2CH_2COO) verified the ester linkage. Thus, all the results showed that PEG side chains were grafted to PMHDO backbone by ester connection.

Generally, ^{1}H NMR can be used to determine the composition of copolymer. In current case, the approximate ratio of total number of EG unit to MHDO unit (N_{EG}/N_{MHDO}) and the grafting density of PEG (N_{PEG}/N_{MHDO}) were calculated from ^{1}H NMR according to eqs 1 and 2 as listed in Table 1 (S_d is the integration area of four protons of OCH_2CH_2 of PEG side chain at 3.64 ppm, S_a is the integration area of six protons of CH(CH_3)$_2$ of PMHDO backbone at 0.88 ppm, 7.36 is the average number of EG unit of PEG side chain),

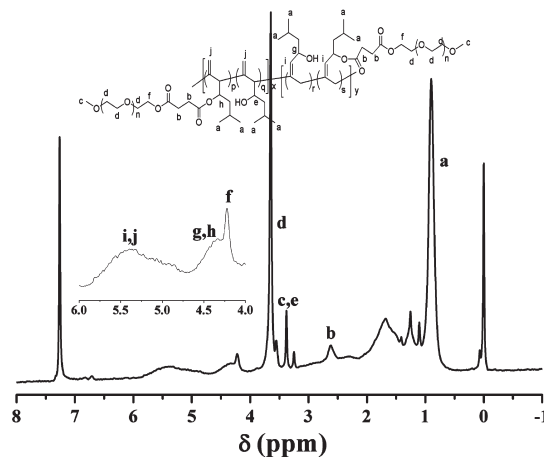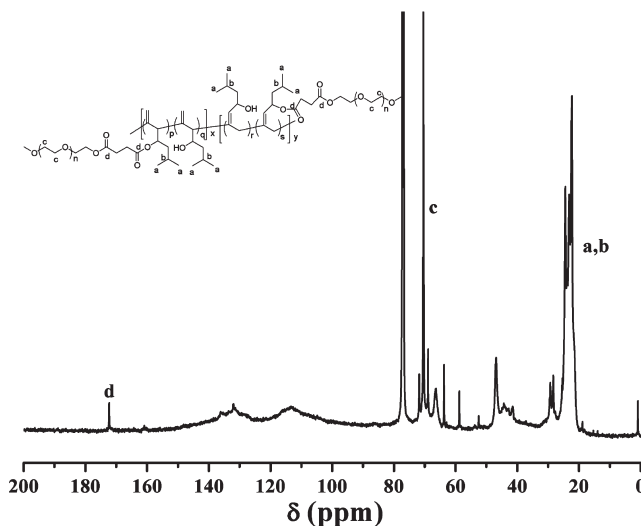**Figure 3.** ^{1}H NMR spectrum of PMHDO-*g*-PEG **4** in CDCl$_3$.

Figure 4. ^{13}C NMR spectrum of PMHDO-*g*-PEG **4** in CDCl$_3$.

respectively. Thus, the molecular weight of graft copolymer ($M_{n,NMR}$) was evaluated according to eq 3 from the value of N_{PEG}/N_{MHDO}, molecular weights of PMHDO backbone (M_n = 5700 g/mol) and CMPEG (M_n = 456 g/mol), and the degree of polymerization of PMHDO backbone (DP = 45). It was found that molecular weight obtained by ^{1}H NMR was higher than that determined by GPC with linear polystyrene standard, which is similar to previous reports.[46,47] In addition, absolute molecular weight of PMHDO-*g*-PEG **4** was measured by light scattering in THF. The result (M_w = 15 000 g/mol) is consistent with the value of molecular weight (M_n = 13 500 g/mol) obtained by ^{1}H NMR, which meant for graft copolymer the molecular weight calculated from ^{1}H NMR was more accurate.

$$N_{EG}/N_{MHDO} = [S_d/4]/[S_a/6] \qquad (1)$$

$$N_{PEG}/N_{MHDO} = [S_d/4]/[7.36 S_a/6] \qquad (2)$$

$$M_{n,NMR} = 5700 + N_{PEG}/N_{MHDO} \times 45 \times 456 \qquad (3)$$

Critical Micelle Concentration. Critical micelle concentration of PMHDO-*g*-PEG **4** amphiphilic graft copolymer in aqueous media was examined by fluorescence technique using PNA as probe. PNA displays higher fluorescence

activity in nonpolar environments, and its fluorescence can be quenched very easily by polar solvents such as water. Furthermore, PNA is a more suitable fluorescent probe than pyrene in terms of reproducibility.[48] The relationship of the fluorescence intensity ratio (I/I_0) of PNA as a function of the concentration of PMHDO-*g*-PEG **4** is shown in Figure 5A. The ratios were almost constant while the concentration was below a certain value. However, I/I_0 increased sharply when the concentration exceeded that value, which showed the incorporation of PNA probe into the hydrophobic region of micelles. Thus, cmc of PMHDO-*g*-PEG **4** was determined to be the intersection of two straight lines with a value of 1.12×10^{-5} g/mL. This value is much lower than those of low molecular weight surfactants; however, it is comparable with those of polymeric amphiphiles.[8-11]

Ion strength is reported to be an important factor to affect the cmc of amphiphilic copolymer.[49] Adding inorganic salt of low molecular weight would increase the ion strength of solution to influence hydrophobic segment, which would make the cmc descend or ascend. In current work, the effect of salt concentration on the cmc was explored in a region between 0 and 0.1 M. The value of cmc quickly dropped while the concentration of NaCl was raised (Figure 5B). When [NaCl] was 0.1 mol/L, the value of cmc fell to 3.09×10^{-6} g/mL. This phenomena can be explained that the addition of NaCl resulted in a salting-out effect on hydrophobic PMHDO segment to increase the hydrophobicity of PMHDO segment so that the hydrophobic segments were easier to aggregate to form micelles and the value of cmc lowered.

Self-Assembled Nanostructures. PMHDO-*g*-PEG **4** is difficult to dissolve in water due to the relative high content of hydrophobic MHDO unit. Therefore, the dialysis method was employed to prepare micelles, PMHDO-*g*-PEG **4** was first dissolved in a small amount of THF followed by adding water (selective solvent for PEG) dropwise to induce self-assembly, and THF was removed by dialysis against deionized water with slow stirring.[50] Micellar morphologies were

visualized under TEM. We first investigated the effect of water content on micellar structures. When water content was kept below 10 wt %, the solution of copolymer kept transparent. Adding more water afforded a bluish solution, which implied the occurrence of self-assembly. Figure 6 show micellar morphologies formed by PMHDO-*g*-PEG **4** with different water contents when the initial concentration of copolymer was 1.6 wt %. The copolymer aggregated to form spherical micelles (ca. 40 nm) with a water content of 14 wt % (Figure 6A). These spherical micelles have a trend to link into cylindrical structures. They changed to coexisted spheres (ca. 25−50 nm) and long cylinders (diameter: ca. 100 nm; length: several micrometers) at a water content of 25 wt % as shown in Figure 6B. On further increasing the water content to 33 wt % (Figure 6C and Figure S1), spheres (ca. 40 nm) can still be observed; however, common cylinders turned into spirally twisted cylinders possessing a diameter of ca. 150 nm and a pitch length of ca. 250 nm though the studied graft copolymer lacks any chiral center in its primary structure. This phenomenon indicated that achiral polymeric architecture could induce helix, which is similar to a previous report.[51] Interestingly, a strong peak at 227 nm attributed to a double bond appeared in the CD spectrum of this solution as shown in Figure 6F, which demonstrated the presence of a chiral source. What is the origin of chiral helical structures? Previous literature has reported that polypropadiene (propadiene is the simplest allene derivative) had a 2_1 helical structure.[52] Every repeating unit of polypropadiene contained a double bond, and this double bond connected to the main chain with a rigid "perpendicular" form, which is the same as our graft copolymer. Thus, we can deduce that these rigid "perpendicular" double bonds may "force" the backbone into an isotactic and/or a syndiotactic configuration. If so, chiral structures would exist along the backbone. Those stereogenic centers may cause a helical bias of the interface of cylindrical micelles.[51] In the current case, a THF/water mixture with a given composition may be a solvophobic solvent for the investigated copolymer, which can help the backbone keep the helical conformation to further induce the formation of helical ribbonlike cylinders. This result demonstrated that double bond may be an important factor of determining micellar morphology. As the water content was increased to 48 wt %, Figure 6D shows a morphological change of converting to exclusively long wormlike micelles. Finally, the water content was increased to 63 wt %, and the morphology transformed into vesicles as shown in Figure 6E. These vesicles have an outer diameter of ca. 500−550 nm and a relatively low polydispersity. The average wall thickness is ca. 100 nm. If more water was added, the morphology did not change again. Thus, micellar

Table 1. Synthesis of PMHDO-*g*-PEG 4 Graft Copolymer[a]

$M_{n,GPC}$[b] (g/mol)	M_w/M_n[b]	$M_{n,NMR}$[c] (g/mol)	N_{EG}/N_{MHDO}[d]	N_{PEG}/N_{MHDO}[e]	cmc[f] (g/mL)
8200	1.22	13 500	125/45	17/45	1.12×10^{-5}

[a] Synthesized from the reaction between PMHDO **1** (M_n = 5700 g/mol, M_w/M_n = 1.17, DP = 45) and CMPEG-Cl **3**. [b] Measured by GPC in THF. [c] Obtained by ^{1}H NMR. [d] The ratio of total number of EG unit to MHDO unit obtained by ^{1}H NMR. [e] The number of PEG side chain grafted onto per MHDO repeating unit obtained by ^{1}H NMR. [f] Critical micelle concentration determined by fluorescence spectroscopy.
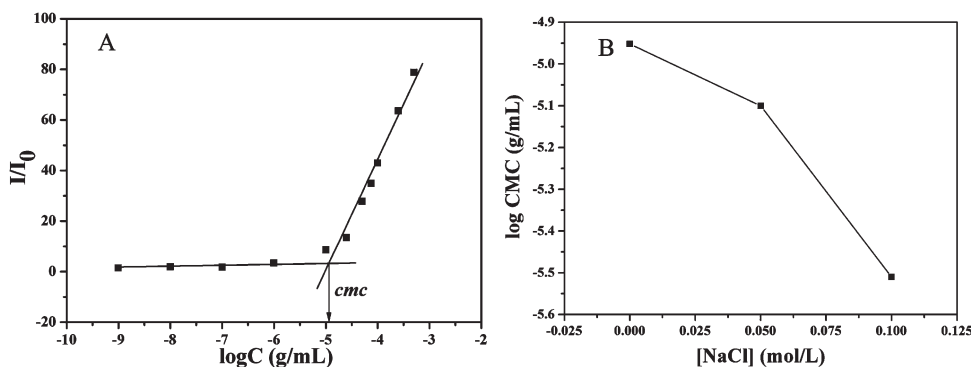

Figure 5. (A) Dependence of fluorescence intensity ratio of PNA emission band at 418 nm on the concentration of PMHDO-*g*-PEG **4** in pure water. (B) Influence of the concentration of NaCl on the cmc of PMHDO-*g*-PEG **4**.
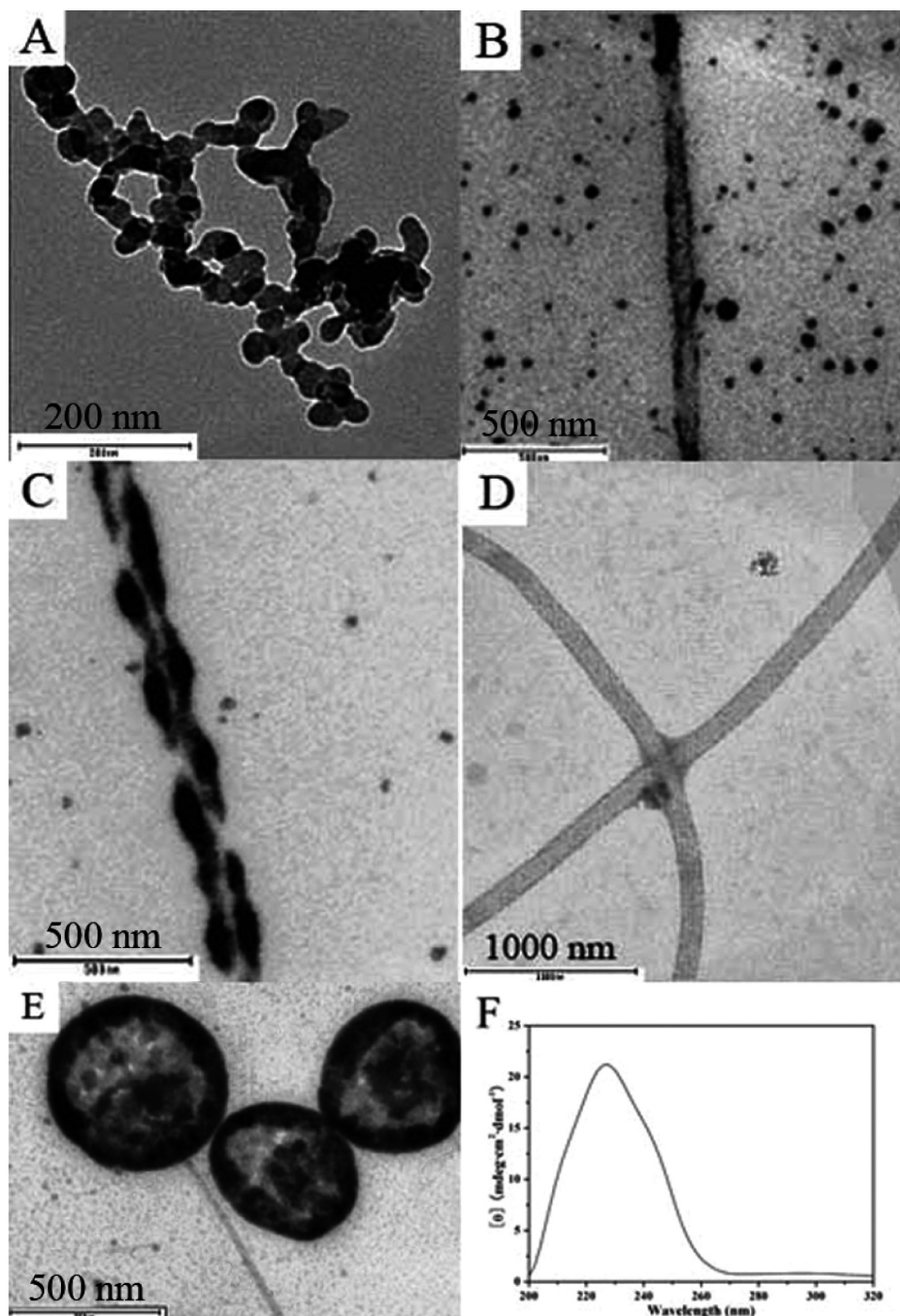
Figure 6. TEM images of micelles formed by PMHDO$_{45}$-*g*-PEG$_{125}$ **4** with different water contents, initial content of graft copolymer in THF: 1.6 wt %, (A) 14, (B) 25, (C) 33, (D) 48, and (E) 63 wt %. (F) CD spectrum of PMHDO$_{45}$-*g*-PEG$_{125}$ **4** with a water content of 33 wt %.

morphologies of PMHDO$_{45}$-*g*-PEG$_{125}$ graft copolymer can be tuned by the water content in a relatively wide range between 14 and 63 wt %.

Next, another four solutions with a low initial copolymer content of 0.1 wt % (water contents were 14, 25, 33, and 63 wt %) were prepared to study the effect of initial content of graft copolymer on micellar structures. When the water content was 14 wt %, the morphology changed to short cylinders with a diameter of ca. 60 nm and a length of ca. 160 nm as shown in Figure 7A compared to spherical micelles with a higher initial copolymer content of 1.6 wt % as shown in Figure 6A. Figure 7B shows coexisted spheres (ca. 90 nm) and short wormlike micelles (diameter: ca. 40 nm;

length: ca. 300 nm) at a water content of 25 wt %; wormlike micelles are completely different from long straight cylinders in Figure 6B. On further increasing the water content to 33 wt % as shown in Figure 7C, we only found dendritic nanofibers with a diameter of ca. 14 nm, and no signal was found in CD spectrum. This result also testified that chiral helical nanostructures can be only induced by achiral copolymer under given conditions. Finally, the morphology was converted to super-rings[51] with relative uniform size while the water content was raised to 63 wt % (Figure 7D). These super-rings have a diameter of ca. 270 nm and a wall thickness of ca. 60 nm. Therefore, it can be concluded that micelle morphology of
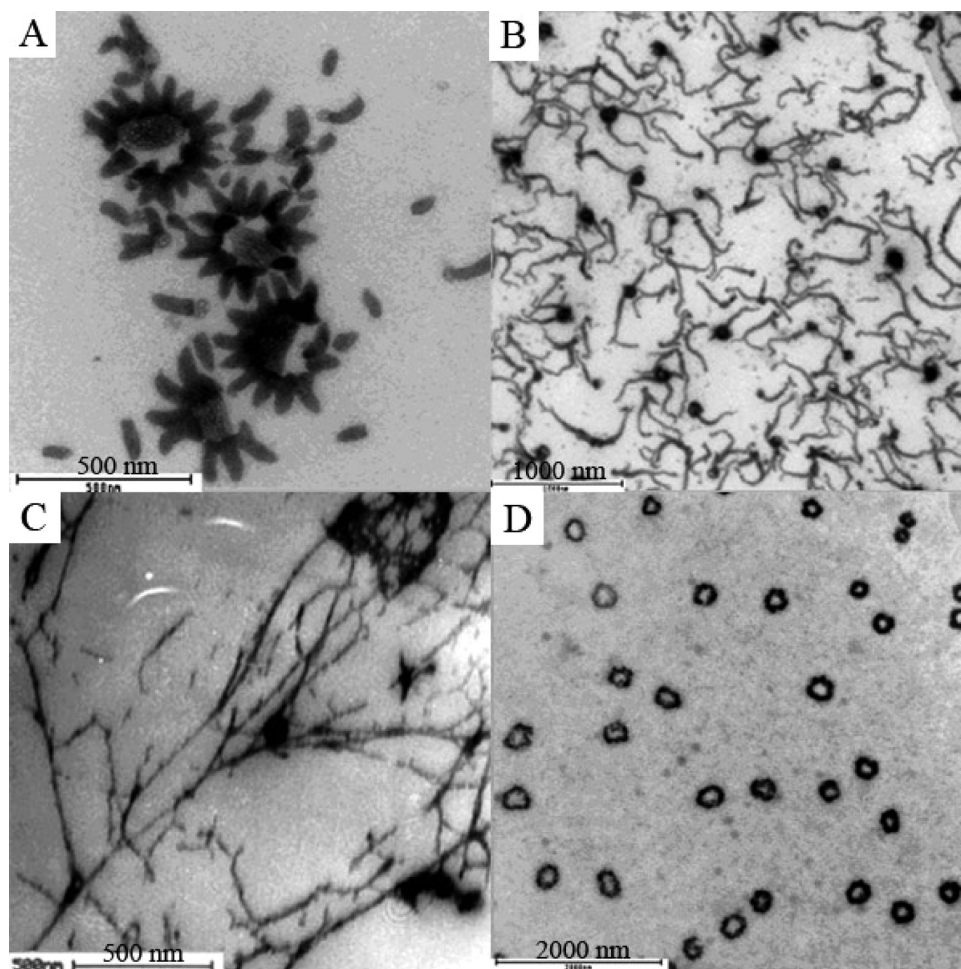
Figure 7. TEM images of micelles formed by $PMHDO_{45}$-g-PEG_{125} **4** with different water contents, initial content of graft copolymer in THF: 0.1 wt %, (A) 14, (B) 25, (C) 33, and (D) 63 wt %.
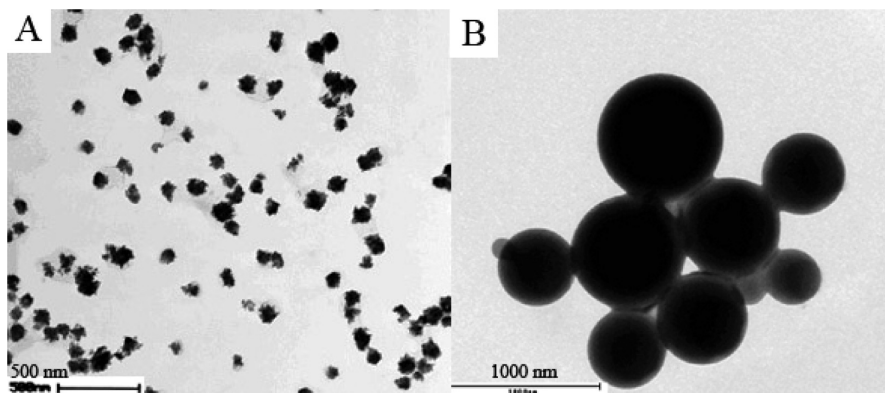

Figure 8. TEM images of micelles formed by $PMHDO_{45}$-g-PEG_{125} **4** with different ion strengths, water content: 14 wt % and initial content of graft copolymer in THF: 1.6 wt %; [NaCl] = 0.05 M (A) and 0.10 M (B).

$PMHDO_{45}$-g-PEG_{125} is also sensitive to the initial copolymer content in THF.

Ion strength was reported to be able to influence micellar morphology and size.[53] Sodium chloride was added to the solution with a water content of 14 wt % and an initial content of graft copolymer of 1.6 wt %. Regular spheres (Figure 6A) turned into irregular spheres with a higher diameter of ca. 80−120 nm with a concentration of NaCl of 0.05 M as shown in Figure 8A. Furthermore, when [NaCl] was increased to 0.10 M, spherical large compound micelles with a diameter of 390−850 nm were found in Figure 8B. This phenomenon can be explained that Na^+ could screen

the repulsion among hydrophilic PEG segments, so the hydrophobic PMHDO segments were easier to aggregate to form big micelles.[53]

Conclusion

In summary, the grafting-onto strategy was employed to synthesize a new double-bond-based amphiphilic graft copolymer containing hydrophilic PEG side chains via coupling reaction between the pendant hydroxyls of PMHDO homopolymer and acyl chloride end group of functionalized MPEG using DMAP as catalyzer. To our best knowledge, this is the first

example of amphiphilic graft copolymer via allene derivative. The cmc of PMHDO-*g*-PEG in aqueous media decreased with the addition of salt. TEM showed diverse micellar morphologies when varying water content, initial copolymer content, and ion strength. In particular, chiral helical twisted cylinders can be induced by PMHDO-*g*-PEG without any chiral center in its primary structure under given conditions. These aggregates may provide templates to fabricate nanocomposites, which is being carried out in our group.

Supporting Information Available: Overview of chiral helical nanostructures. This material is available free of charge via the Internet at http://pubs.acs.org.

References and Notes

(1) Zhang, L. F.; Eisenberg, A. *Macromolecules* **1996**, *29*, 8805–8815.
(2) Zhang, L. F.; Yu, K.; Eisenberg, A. *Science* **1996**, *272*, 1777–1779.
(3) Xu, R. L.; Winnik, M. A.; Hallett, F. R.; Riess, G.; Croucher, M. D. *Macromolecules* **1991**, *24*, 87–93.
(4) Pan, D.; Turner, J. L.; Wooley, K. L. *Chem. Commun.* **2003**, 2400–2401.
(5) Kataoka, K. *J. Macromol. Sci., Pure Appl. Chem.* **1994**, *A31*, 1759–1769.
(6) Rosler, A.; Vandermeulen, G. W. M.; Klok, H. A. *Adv. Drug Delivery Rev.* **2001**, *53*, 95–108.
(7) Ahmed, F.; Discher, D. E. *J. Controlled Release* **2004**, *96*, 37–53.
(8) Clendenning, S. B.; Fournier-Bidoz, S.; Pietrangelo, A.; Yang, G. C.; Han, S. J.; Brodersen, P. M.; Yip, C. M.; Lu, Z. H.; Ozin, G. A.; Manners, I. *J. Mater. Chem.* **2004**, *14*, 1686–1690.
(9) Whitesides, G. M.; Grzybowski, B. *Science* **2002**, *295*, 2418–2421.
(10) Ruokolainen, J.; Makinen, R.; Torkkeli, M.; Makela, T.; Serimaa, R.; Brinke, G. T.; Ikkala, O. *Science* **1998**, *280*, 557–560.
(11) Thurmond, K. B.; Kowalewski, T.; Wooley, K. L. *J. Am. Chem. Soc.* **1997**, *119*, 6656–6665.
(12) Maskos, M.; Harris, J. R. *Macromol. Rapid Commun.* **2001**, *22*, 271–273.
(13) Forder, C.; Patrickios, C. S.; Armes, S. P.; Billingham, N. C. *Macromolecules* **1996**, *29*, 8160–8169.
(14) Xu, Z. S.; Yi, C. F.; Cheng, S. Y.; Feng, L. X. *Polym. Bull.* **2000**, *44*, 215–222.
(15) Booth, C.; Attwood, D. *Macromol. Rapid Commun.* **2000**, *21*, 501–527.
(16) Ma, Y. H.; Cao, T.; Webber, S. E. *Macromolecules* **1998**, *31*, 1773–1778.
(17) Riess, G. *Prog. Polym. Sci.* **2003**, *28*, 1107–1170.
(18) Cai, Y. L.; Tang, Y. Q.; Armes, S. P. *Macromolecules* **2004**, *37*, 9728–9737.
(19) Forster, S.; Plantenberg, T. *Angew. Chem., Int. Ed.* **2002**, *41*, 688–714.
(20) Zhang, M.; Breiner, T.; Mori, H.; Muller, A. H. E. *Polymer* **2003**, *44*, 1449–1458.
(21) Dziezok, P.; Sheiko, S. S.; Fischer, K.; Schmidt, M.; Moller, M. *Angew. Chem., Int. Ed.* **1997**, *36*, 2812–2815.
(22) Heroguez, V.; Gnanou, Y.; Fontanille, M. *Macromolecules* **1997**, *30*, 4791–4798.
(23) Beers, K. L.; Gaynor, S. G.; Matyjaszewski, K.; Sheiko, S. S.; Moller, M. *Macromolecules* **1998**, *31*, 9413–9415.
(24) Wang, J. S.; Matyjaszewski, K. *Macromolecules* **1995**, *28*, 7901–7910.
(25) Percec, V.; Barboiu, B. *Macromolecules* **1995**, *28*, 7970–7972.
(26) Kato, M.; Kamigaito, M.; Sawamoto, M.; Higashimura, T. *Macromolecules* **1995**, *28*, 1721–1723.
(27) Percec, V.; Guliashvili, T.; Ladislaw, J. S.; Wistrand, A.; Stjerndahl, A.; Sienkowska, M. J.; Monteiro, M. J.; Sahoo, S. *J. Am. Chem. Soc.* **2006**, *128*, 14156–14165.
(28) Moad, G.; Rizzardo, E.; Thang, S. H. *Polymer* **2008**, *49*, 1079–1131.
(29) Yamada, K.; Miyazaki, M.; Minoda, M. *Macromolecules* **1999**, *32*, 290–293.
(30) Zhang, D.; Macias, C.; Ortiz, C. *Macromolecules* **2005**, *38*, 2530–2534.
(31) Hong, S. C.; Jia, S.; Teodorescu, M.; Kowalewski, T.; Matyjaszewski, K.; Gottfried, A. C.; Brookhart, M. *J. Polym. Sci., Polym. Chem.* **2002**, *40*, 2736–2749.
(32) Matyjaszewski, K.; Xia, J. *Chem. Rev.* **2001**, *101*, 2921–2990.
(33) Deffieux, A.; Schappacher, M. *Macromolecules* **1999**, *32*, 1797–1802.
(34) Endo, T.; Tomita, I. *Prog. Polym. Sci.* **1997**, *22*, 565–600.
(35) Tomita, I.; Kondo, Y.; Takagi, K.; Endo, T. *Macromolecules* **1994**, *27*, 4413–4414.
(36) Takagi, K.; Tomita, I.; Endo, T. *Macromolecules* **1997**, *30*, 7386–7390.
(37) Takagi, K.; Tomita, I.; Endo, T. *Macromolecules* **1998**, *31*, 6741–6747.
(38) Taguchi, M.; Tomita, I.; Endo, T. *Angew. Chem., Int. Ed.* **2000**, *39*, 3667–3669.
(39) Kyohei, M.; Tomita, I. *Macromolecules* **2006**, *39*, 6336–6340.
(40) Zhang, X. H.; Peng, D.; Lu, G. L.; Gu, L. N.; Huang, X. Y. *J. Polym. Sci., Polym. Chem.* **2006**, *44*, 6888–6893.
(41) Zhang, X. H.; Shen, Z.; Li, L. T.; Zhang, S.; Lu, G. L.; Huang, X. Y. *J. Polym. Sci., Polym. Chem.* **2007**, *45*, 5509–5517.
(42) Zhang, X. H.; Shen, Z.; Li, L. T.; Lu, G. L.; Gu, L. N.; Huang, X. Y. *Polymer* **2007**, *48*, 5507–5513.
(43) Shimizu, S.; Sugiura, T.; Tsuji, T. *J. Org. Chem.* **1985**, *50*, 537–539.
(44) Park, S. Y.; Han, D. K.; Kim, S. C. *Macromolecules* **2001**, *34*, 8821–8824.
(45) Parrish, B.; Emrick, T. *Macromolecules* **2004**, *37*, 5863–5865.
(46) Jia, Z.; Fu, Q.; Huang, J. *Macromolecules* **2006**, *39*, 5190–5193.
(47) Peng, D.; Zhang, X. H.; Huang, X. Y. *Macromolecules* **2006**, *39*, 4945–4947.
(48) Xu, P. S.; Tang, H. D.; Li, S. Y.; Ren, J.; Van Kirk, E.; Murdoch, W. J.; Radosz, M.; Shen, Y. Q. *Biomacromolecules* **2004**, *5*, 1736–1744.
(49) Astafieva, I.; Khougaz, K.; Eisenberg, A. *Macromolecules* **1995**, *28*, 7127–7134.
(50) Bhargava, P.; Zheng, J. X.; Li, P.; Quirk, R. P.; Harris, F. W.; Cheng, S. Z. D. *Macromolecules* **2006**, *39*, 4880–4888.
(51) Cheng, H. X.; Huang, Y.; Tang, R. P.; Chen, E. Q.; Xi, F. *Macromolecules* **2005**, *38*, 3044–3047.
(52) Otsuka, S.; Mori, K.; Imaizumi, F. *J. Am. Chem. Soc.* **1965**, *87*, 3017–3019.
(53) Ma, Y.; Cao, T.; Webber, S. E. *Macromolecules* **1998**, *31*, 1773–1778.